Lehigh University
Lehigh Preserve

Theses and Dissertations

1-1-1983

Ultrasonic and mechanical properties of some iron-based binary alloys.

Surin Tanticharoenkiat

Follow this and additional works at: http://preserve.lehigh.edu/etd

 Part of the Materials Science and Engineering Commons

Recommended Citation
Tanticharoenkiat, Surin, "Ultrasonic and mechanical properties of some iron-based binary alloys." (1983). *Theses and Dissertations.* Paper 1935.

This Thesis is brought to you for free and open access by Lehigh Preserve. It has been accepted for inclusion in Theses and Dissertations by an authorized administrator of Lehigh Preserve. For more information, please contact preserve@lehigh.edu.

ULTRASONIC AND MECHANICAL PROPERTIES

OF SOME IRON-BASED BINARY ALLOYS

by

Surin Tantitharoenkiat

A Thesis

Presented to the Graduate Commitee

of Lehigh University

in Candidacy for the Degree of

Master of Science

in

Metallurgy and Materials Engineering

Lehigh University

1983

ProQuest Number: EP76208

All rights reserved

INFORMATION TO ALL USERS
The quality of this reproduction is dependent upon the quality of the copy submitted.

In the unlikely event that the author did not send a complete manuscript
and there are missing pages, these will be noted. Also, if material had to be removed,
a note will indicate the deletion.

ProQuest EP76208

Published by ProQuest LLC (2015). Copyright of the Dissertation is held by the Author.

All rights reserved.
This work is protected against unauthorized copying under Title 17, United States Code
Microform Edition © ProQuest LLC.

ProQuest LLC.
789 East Eisenhower Parkway
P.O. Box 1346
Ann Arbor, MI 48106 - 1346

CERTIFICATE OF APPROVAL

This thesis is accepted in partial fulfillment of the requirements for the degree of Master of Science.

Dec. 9, 1983
(date)

Professor in Charge

Chairman of the Department

ACKNOWLEDGEMENT

The author acknowledges a deep sense of gratitude to Dr. Y. T. Chou for his support during the course of this work. He is grateful to Dr. N. Eberhardt, Dr. M. Deka and Joseph A. Bohar for their work on ultrasonic measurements and for their helpful suggestions. Thanks are due to Srinivasarao Lathabai for her help on micrographs preparation.

Finally, the author acknowledges the financial support of this research program by Bethlehem Steel,Inc. and Lehigh University for its support through the Distinguished Fellowship.

TABLE OF CONTENTS

	Page
CERTIFICATE OF APPROVAL	ii
ACKNOWLEDGEMENT	iii
LIST OF TABLES	v
LIST OF FIGURES	vi
ABSTRACT	1
I. INTRODUCTION	3
II. SAMPLE PREPARATION & MECHANICAL TESTING	5
Materials	5
Heat Treatment	8
Mechanical Testing	13
III. ULTRASONIC TESTING	17
Method of Measurement	17
Measurement under Magnetic Saturation	21
Effect of Residual Strain	25
IV. RESULTS AND DISCUSSIONS	28
Electrolytic Iron & 0.035 % C Steel	30
Fe-Cr Steel	30
Fe-Si Steel	38
Fe-Mo Steel	44
Fe-P Steel	44
Effect of Alloying Elements	53
V. CONCLUSIONS	56
REFERENCES	58
VITA	60

LIST OF TABLES

No.	Description	Page
1	Materials and their Chemical Analysis	6
2	Procedure of Heat Treatment	9
3	Mechanical Test Data for Electrolytic Iron	33
4	Mechanical Test Data for Fe-0.035 % C Steel	34
5	Mechanical Test Data for Fe-3.8 % Cr Steel	40
6	Mechanical Test Data for Fe-7.8 % Cr Steel	40
7	Mechanical Test Data for Fe-0.8 % Si Steel	43
8	Mechanical Test Data for Fe-1.5 % Si Steel	43
9	Mechanical Test Data for Fe-1.36 % Mo Steel	48
10	Mechanical Test Data for Fe-3.6 % Mo Steel	48
11	Mechanical Test Data for Fe-0.08 % P Steel	52
12	Mechanical Test Data for Fe-0.28 % P Steel	52

LIST OF FIGURES

No.	Description	Page
1	Flow Chart of Sample Preparation	7
2	Micrograph of 3.6 % Mo Steel, Heat Treated at 500 °C, 1 Hour	11
3	Micrograph of 3.6 % Mo Steel, Heat Treated at 900 °C, 1 Hour	11
4	Micrograph of 3.6 % Mo Steel, Heat Treated at 1100 °C, 1 Hour	12
5	Micrograph of 3.6 % Mo Steel, Heat Treated at 1200 °C, 1 Hour	12
6	Sub-Size Rectangular Tension Test Specimen	15
7	Small-Size Round Tension Test Specimen	16
8	Cylindrical Ultrasonic Resonator Coupled to Shear Wave Transducers	19
9	Block Diagram of The Experimental Set Up	20
10	Configuration for Measurement under Magnetic Saturation	23
11	Decline of Q_t^{-1} in Fe-7.8 % Cr with Increasing Magnet Current	24
12	Q_t^{-1} in Fe and Fe-7.8 % Cr No Magnetic Field & Magnetic Saturation	24
13	Drop of Q_t^{-1} after Successive Compression of Cylinder with Increasing Force.	27
14	Drop of Initial Permeability after Successive Compression of Cylinder with Increasing Force	27
15	Attenuation in Electrolytic Iron	31
16	Attenuation in Fe-0.035 % C Steel	31

No.	Description	Page
17	Curvefit to Hall-Petch Relation Fe and Fe-0.035 % C Steel	32
18	Attenuation in Fe-7.8 % Cr	36
19	Attenuation in Fe-7.8 % Cr Alternate Specimen	36
20	Attenuation in Fe-3.8 % Cr	37
21	Hardness vs. Shear Velocity in Fe-Cr Steel	37
22	Curvefit to Hall-Petch Relation Fe-3.8 % Cr and Fe-7.8 % Cr Steels	39
23	Attenuation in Fe-0.8 % Si Steel	41
24	Attenuation in Fe-1.5 % Si Steel	41
25	Curvefit to Hall-Petch Relation Fe-0.8 % Si and Fe-1.5 % Si Steels	42
26	Attenuation in Fe-1.5 % Mo Steel	45
27	Attenuation in Fe-3.6 % Mo Steel	45
28	Hardness vs. Shear Velocity in Fe-Mo Steel	46
29	Curvefit to Hall-Petch Relation Fe-1.36 % Mo and Fe-3.6 % Mo Steels	47
30	Attenuation in Fe-0.08 % P Steel	49
31	Attenuation in Fe-0.28 % P Steel	49
32	Hardness vs. Shear Velocity in Fe-P Steel	50
33	Curvefit to Hall-Petch Relation Fe-0.08 % P and Fe-0.28 % P Steels	51

ABSTRACT

Samples of electrolytic iron, Fe-Cr, Fe-Si, Fe-Mo, Fe-C, and Fe-P alloy steels were prepared for ultrasonic and mechanical testing. Methods and detailed procedures in the preparation of samples with varying grain sizes are reported, together with data on yield strength, ultimate tensile strength, percent reduction of area and Rockwell hardness.

A newly developed resonance method was used to measure the ultrasonic velocities and their attenuations up to a few MHz. Measurements are employed for both longitudinal and transverse modes. Data are also presented on velocities of transverse and longitudinal waves.

It is found that the predominant mechanism of absorption is magnetoelastic in nature (micro eddycurrent loss). Also the absorption is mostly due to the shear viscosity coefficent which is found to be much larger than the bulk viscosity coefficent. There is a strong influence of small coldwork or residual strain. In the alloys where initial permeability and absorption were measured as function of coldwork, a direct proportionality between permeability and absorption was found.

Some characteristic grain size dependence of absroption exists in Fe-Si and Fe-P alloy steels, otherwise absorption is dependent on other, as yet unknown, microscopic properties within the grain; no distinct grain size dependence was observed.

Correlations to yield strength, tensile strength and hardness can not be convincingly demonstrated in any of the data except in Fe-Si and Fe-P alloy steels, where the frequency of the absorption peak is grain size dependent.

I. INTRODUCTION

The initial objectives of this research were to provide new fundamental information on the influence of microstructure (in particular the grain size) and alloy compositions on the ultrasonic material parameters, namely the ultrasonic velocities (longitudinal and transverse) and the attenuations of longitudinal and transverse waves. If there exists a correlation between grain size and ultrasonic parameters, then via the well established dependence of mechanical properties (the yield strength) on grain size (the Hall-Petch relation), ultrasonic measurements can be used as a new nondestructive method to measure the mechanical properties of materials.

A resonance method was used to measure the ultrasonic parameters. This insures that the absorption is clearly separated from the scattering and also that longitudinal waves and their absorptions are clearly separated from the transverse waves. A new techique was also used to measure absorption under magnetic saturation, so as to exclude the magnetoelastic (micro eddycurrent) part of absorption.

In order not to complicate things too much at first, a dicision was made to investigate only electrolytic iron and binary alloy steels. Five different alloy steels (Fe-Cr, Fe-Si, Fe-Mo, Fe-C and Fe-P) were choosen.

Except for Fe-C steel each alloy steels were provided with two different concentrations by Bethlehem Steel. After some initial difficulties with growing different grain sizes in some alloy steels, we manage to get three or four grain sizes on each set of the alloy steels. Thus we could work with variety of materials and collect a significant amount of both mechanical and ultrasonic data for comparison and correlation.

As the work progressed, it became clear that grain size had a relatively insignificant influence on ultrasonic absorption. The ultrasonic velocities were not strongly influecned by grain size. It was also found that ultrasonic absorption had a strong dependence on small amount of coldwork. In this report ultrasonic data will be presented and will be correlated to measured mechanical parameters.

II. SAMPLE PREPARATION & MECHANICAL TESTING

Materials

One sample of electrolytic iron and 10 binary alloy steels were prepared by Bethlehem Steel. The alloy compositions of these steels are given in Table 1. The initial materials were in slab form, both hot rolled and cold rolled. The forming process, shown in figure 1, is described as follows: An 150 lb. ingot of alloy was vacuum melted, using electrolytic iron as the base metal. Then it was slabbed to a thickness of 0.75 inch, hot rolled down to 0.5 inch and finally cold rolled down 20% to 0.4 inch. After this it was heat treated. The size of each slab is approximately 6 inches wide. The samples were cut from these slabs to approximately 1 inch wide, 6 inches long and same thickness as in the initial condition. Cutting was done parallel to the width of the initial slab. A small sample was taken prior to the heat treatment for the microstructure examination and another sample after the heat treatment. If the structure is equiaxed and uniform, the sample is then further processed for grain size measurement, ultrasonic and mechanical testing.

Table 1. Materials and their Chemical Analysis (wt.%).

Specimen	C	Mn	P	S	Si	Ni	Cr	Mo	Cu	Sn	Al	V	Ti	Cb
E. Iron 48A	.005	.01	.002	.005	.01	.01	.01	.02	.005	.002	.005	.002	.002	.005
0.035 % C 48B	.035	.01	.002	.005	.01	.01	.01	.02	.005	.002	.005	.002	.002	.005
0.8 % Si T024	.011	.08	.002	.004	.80	.01	.01	.02	.005	.002	.010	.002	.003	.005
1.5 % Si 50A	.011	.08	.002	.004	1.50	.01	.01	.02	.005	.002	.010	.002	.003	.005
1.36 % Mo T023	.007	.01	.002	.005	.07	.01	.01	1.36	.005	.002		.002	.002	
3.6 % Mo 51A	.007	.01	.002	.005	.07	.01	.01	3.6	.005	.002		.002	.002	
0.082 % P T022	.004	.01	.082	.004	.01	.01	.01	.02	.005	.002	.005	.005	.003	.005
0.28 % P 52A	.004	.01	.28	.004	.01	.01	.01	.02	.005	.002	.005	.005	.003	.005
3.8 % Cr T025	.003	.01	.003	.005	.014	.024	3.8	.02	.005	.002	.005	.002	.002	.005
7.8 % Cr 54B	.003	.02	.004	.005	.025	.023	7.8	.02	.005	.002	.005	.003	.003	.005

SAMPLE PROCESSING

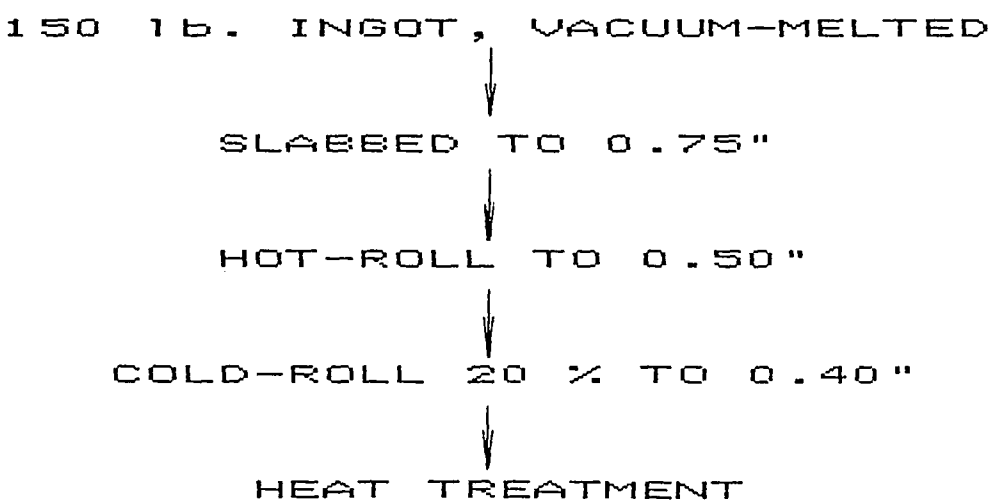

Figure 1. Flow Chart of Sample Preparation.

Heat Treatment

The heat treatments were done in an argon atmosphere furnace with the heating rate of about 150 °C per hour. The initial samples were either cut from the hot rolled or cold rolled slabs depending on which is more appropriate, eg. the uniformity of the initial slab. The details of each heat treatment are given in Table 2. After the heat treatment the piece was cut into two halves, one for the ultrasonic measurement and the other for the grain size measurement and mechanical testing. Grain size measurement was done using the planimetric (or Jeffries) method (counting the grains within a known area circle). After the heat treatment all of the samples have uniform and equiaxed grains. Examples of micrographs are shown in Figures 2-5 (3.6 % Mo Steel).

Table 2. Procedure of Heat Treatment.

Sample #	Grain size mm.	Initial form *	Temp. °C	Time at Temp. hrs.	Cooling rate.
Electrolytic Iron					
18	0.057	H	950	one hour, air cool twice	(double normalizing)
20	0.086	H	950	1	furnace cool
22	0.100	H	1000	3	furnace cool
26	0.120	H	1000	24	furnace cool
0.035 % C Steel					
17	0.038	H	950	one hour, air cool twice	(double normalizing)
21	0.056	H	950	1	furnace cool
23	0.086	H	1000	6	furnace cool
32	0.097	H	1000	12	furnace cool
0.8 % Si Steel					
54	0.074	H	500	1	furnace cool
53	0.087	H	1000	1	furnace cool
54	0.107	C	1000	8	furnace cool
1.5 % Si Steel					
24	0.041	C	500	1	furnace cool
19	0.087	C	950	1	furnace cool
27	0.157	C	1100	2	furnace cool
25	0.186	C	1300	4	furnace cool
1.36 % Mo Steel					
45	0.044	H	700	1	furnace cool
44	0.053	H	850	1	furnace cool
47	0.096	C	900	1	furnace cool
46	0.132	C	1000	2	furnace cool

Table 2. Procedure of Heat Treatment (continued).

Sample #	Grain size mm.	Initial form *	Temp. °C	Time at Temp. hrs.	Cooling rate.
3.6 % Mo Steel					
28	0.053	C	500	1	furnace cooled
29	0.075	H	900	1	furnace cooled
30	0.167	C	1100	1	furnace cooled
31	0.219	C	1200	1	furnace cooled
0.082 % P Steel					
51	0.072	H	800	1	furnace cooled
50	0.088	H	900	2	furnace cooled
49	0.110	H	1000	1	furnace cooled
48	0.124	H	1000	4	furnace cooled
0.28 % P Steel					
38	0.106	C	500	1	furnace cooled
39	0.277	C	1000	1	furnace cooled
40	0.306	C	1200	1	furnace cooled
3.8 % Cr Steel					
35	0.032	H	500	1	furnace cooled
37	0.051	H	700	1	air cooled
36	0.161	H	900	4	furnace cooled
7.8 % Cr Steel					
12	0.035	H	500	1	furnace cooled
15	0.057	H	825	1	air cooled
13	0.095	H	900	1	furnace cooled
14	0.138	H	950	2	furnace cooled

* C = cold rolled H = hot rolled

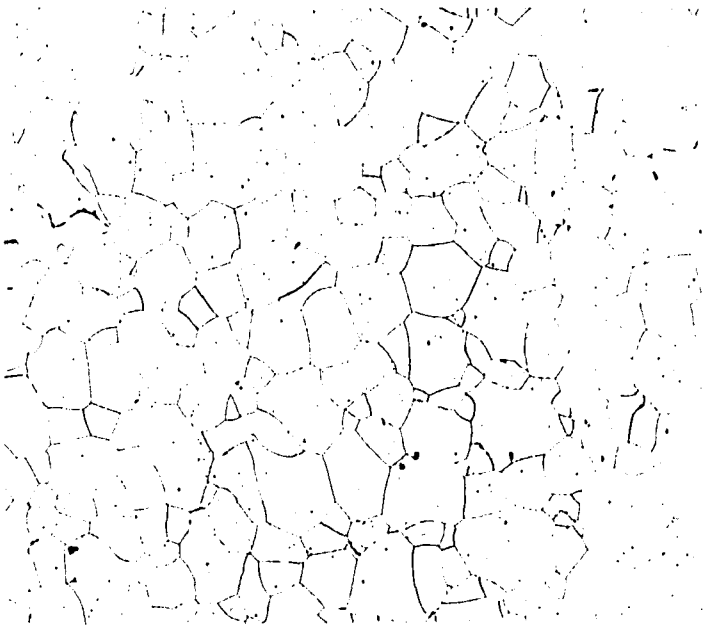

Figure 2. Micrograph of 3.6 % Mo Steel, Heat Treated at 500 °C for 1 Hour and Furnace Cool. Mag. 100x

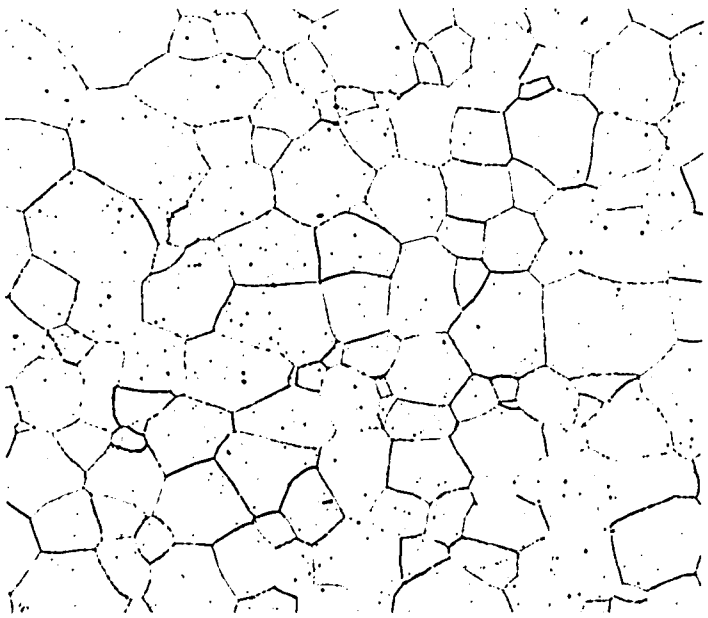

Figure 3. Micrograph of 3.6 % Mo Steel, Heat Treated at 900 °C for 1 Hour and Furnace Cool. Mag. 100x

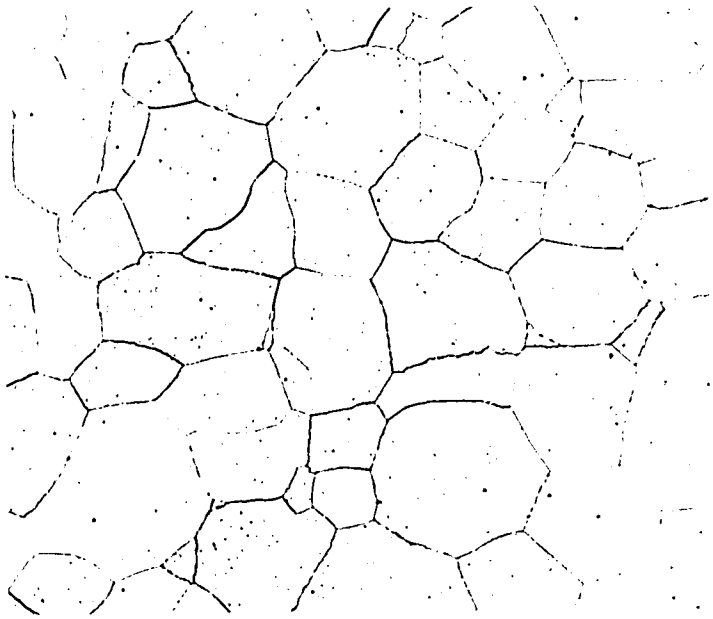

Figure 4. Micrograph of 3.6 % Mo Steel, Heat Treated at 1100°C for 1 Hour and Furnace Cool. Mag. 100x

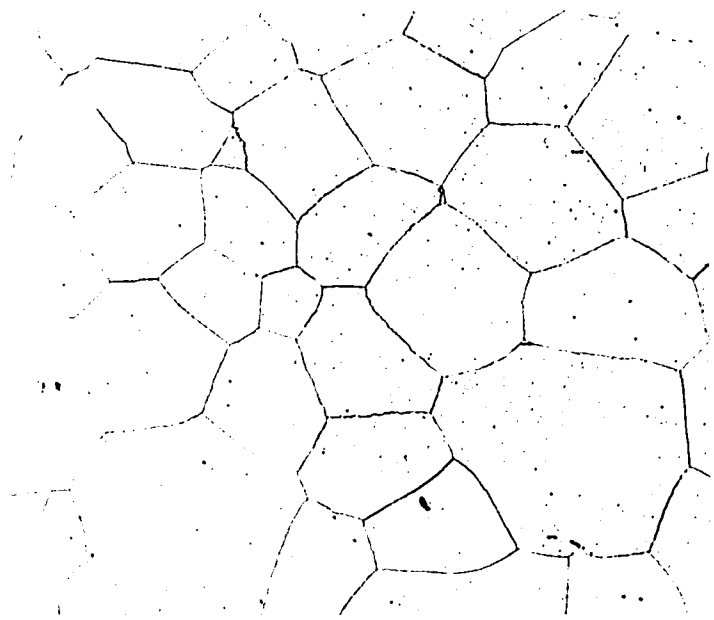

Figure 5. Micrograph of 3.6 % Mo Steel, Heat Treated at 1200°C for 1 Hour and Furnace Cool. Mag. 100x

Mechanical Testing

In order to obtain the mechanical data, a series of specimens were made from each set of the steels. Two types of testing were used, (1) tension test and (2) hardness test.

Specimen Preparation

Two types of specimens were used for the tension test. The sub-size rectangular tension test specimen and the small-size round tension test specimen. These are shown in figures 6 and 7. The 0.28 % P steel (No. 38, 39, 40), 0.08 % P (No. 48, 49, 50, 51), 1.36 % Mo steel (No. 44, 45, 46, 47) and the 0.8 % Si steel (No. 52, 53, 54) are small-size round tension specimens and the rest are sub-size rectangular tension specimens.

Testing Procedure

After machining, each specimen was annealed at 500 °C for one hour. Then before the tension test, the hardness test was made on the grip section of the specimen. Five measurements were made on each specimen and the average value was used. Except for the electrolytic iron and 0.035 % C steel, which were tested using Rockwell E scale, the rest was tested using Rockwell B scale. The size of each specimen was measured before the tension test.

The tension test was done using an Instron machine at a constant strain rate of 0.5 inch per minute. After the test,the size of each specimen was measured again. The mechanical data are given in section IV together with the ultrasonic data.

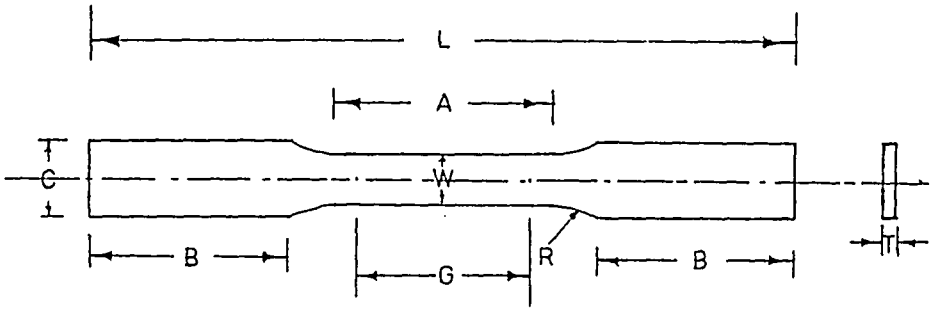

G : Gage length	=	1.00	inch
W : Width	=	0.25	inch
T : Thickness	=	0.125	inch
R : Radius of fillet, min.	=	0.25	inch
L : Overall length	=	4.00	inch
A : Length of the reduce section	=	1.25	inch
B : Length of grip section	=	1.25	inch
C : Width of grip section	=	0.375	inch

Figure 6. Sub-size Rectangular Tension Test Specimen.

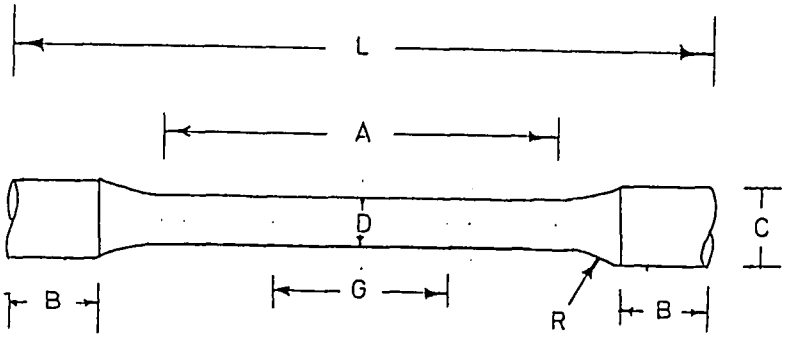

G : Gage length	= 1.00	inch
D : Diameter	= 0.25	inch
R : Radius of fillet, min.	= 0.1875	inch
L : Overall length	= 4.00	inch
A : Length of the reduce section	= 1.25	inch
B : Length of grip section	= 0.50	inch
C : Width of grip section	= 0.375	inch

Figure 7. Small-size Round Tension Test Specimen.

III. ULTRASONIC TESTING

Method of Measurement

A resonance method (1,2) with some simplifications was used to measure the ultrasonic velocities and the attenuations in the frequency range from 100 KHZ to about 2 MHZ. In principle we measure the transmission spectrum through loosely coupled cylindrical resonators made from the material to be investigated. Each cylinder was carefully annealed prior to the measurement to eliminate (minimize) any coldwork effect which could be caused during the machining process. Commercial broadband shear-wave transducers were used. One successful way of loosely coupling is as follows (see figure 8): steel spheres of 0.3 mm diameter (from ball point pens) are honed down to half-spheres. The cylindrical resonators are being contacted in two points by the half-spheres. The choice of the location of the contact point is essential. It is possible to verify vibrational patterns of a given mode of vibration by contacting at various points along the cylinders, using various orientations (with respect to polarization) and monitoring the transmitted signal at resonance. A combination of a small pressure and choice of the contact points near a vibrational node leads to sufficiently loose coupling and thus insures a large

external Q-factor, Q_e. The full transmission bandwidth is equal to Q_L^{-1}, the inverse loaded Q. The general relation $Q_L^{-1} = Q_e^{-1} + Q_o^{-1}$ exists. Q_o, the internal Q, is the quantity to be measured, hence the need to minimize Q_e^{-1}. The transmission test set is computer-controlled with automatic curve fitting and determination of $Q_L^{-1} \cong Q_o^{-1}$. A block diagram of the test set is given in figure 9. An internal Q factor will be designated by either Q_t or Q_l, depending on whether standing transverse or longitudinal waves are involved.

To measure the absorption and velocity of purely transverse waves (vibrations), torsional modes were used. Their resonant frequencies are given by the simple condition that the length of the cylinder be an integer multiple of $\lambda/2$ where λ is the wavelength of shear-waves. Hence only the shear-modulus is involved. The inverse full bandwidth of such modes gives the transverse Q, Q_t directly.

To measure the absorptoin and velocity of longitudinal vibrations, cylinders of aspect ratio one (diameter = height) were used. This gives a resonance that almost exclusively depends on the longitudinal velocity alone. Thus the Q-factor of this resonance is directly the longitudinal Q, Q_l. This is an almost compressional mode and is used to determine Q_l and V_l.

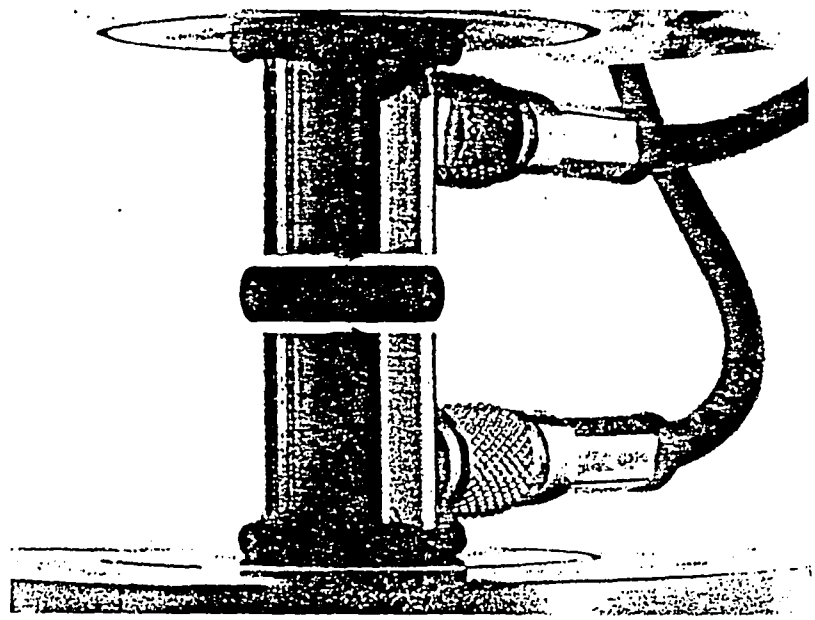

Figure 8. Cylindrical Ultrasonic Resonator Coupled to Shear Wave Transducers.

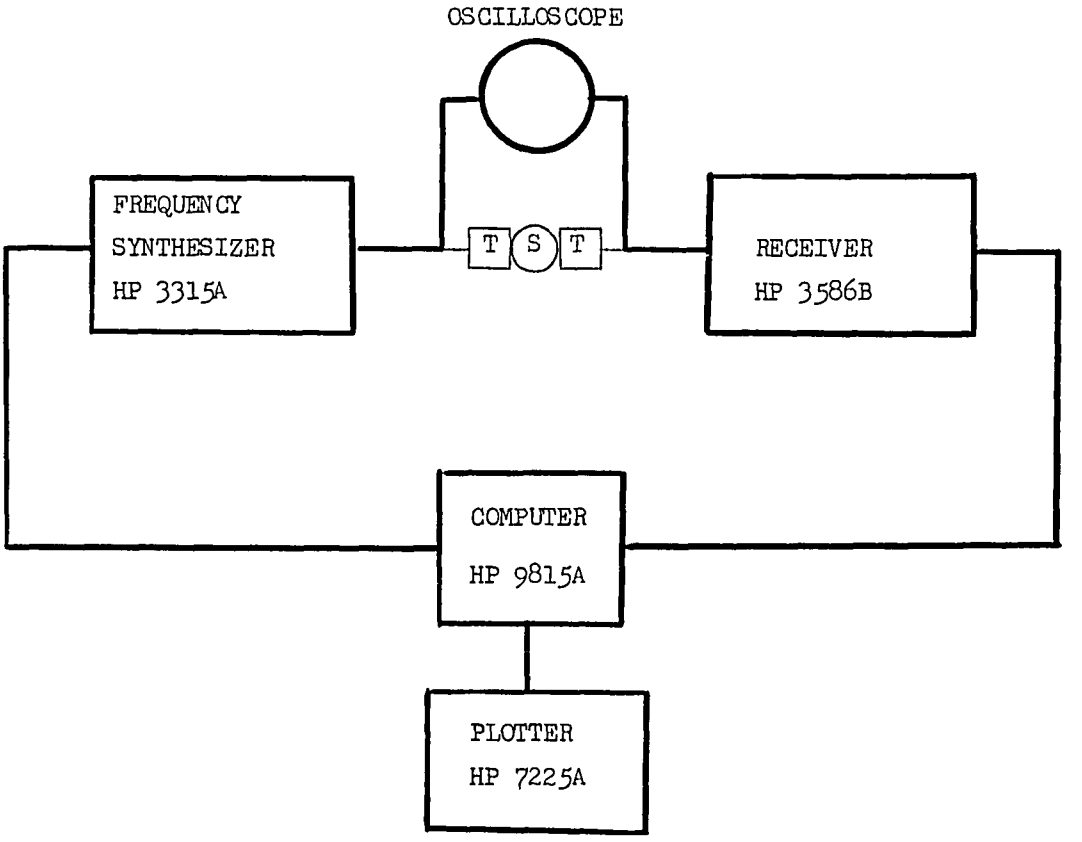

Figure 9. Block Diagram of the Experimental Set Up.

Measurement under Magnetic Saturation

In order to separate the magnetoelastic part from other sources of absorption, the standard measurements were repeated under magnetic saturation on a set of alloy steel (7.8 % Cr). A picture of set up is shown in figure 10. An electromagnet induces a horizontal magnetic flux through the ultrasonic resonator. One difficulty arises from the fact that additional contact points are necessary in order to counteract the magnetic forces which tend to close the airgap between the resonator and the polepiece. Styrofoam pads and axial pins were used to separate the resonator. This however causes an additional external loading and bring the value of Q_e^{-1} up to around 2 to 5×10^{-4}. This is also the limit of all measured Q_t^{-1} under magnetic saturation. It can be concluded that the non-magnetoelastic background of absorption in all measured specimen is given by $Q_t^{-1} \leq 5 \times 10^{-4}$. In practice this means that in all samples the non-magnetoelastic part of absorption is found to be small as compared to the magnetoelastic part.

Figure 11 shows an example of measured values of Q_t^{-1} as the magnet current increases. The plateau of the curve at the higher magnet current is correspondent to magnetic saturation.

Figure 12 shows Q_l^{-1} versus frequency in electrolytic iron and Fe-7.8 % Cr steel, as taken without magnetic field and under magnetic saturation. The saturated curves for both electrolytic iron and the Fe-7.8 % Cr steel are essentially the same and correspond to the instrument limit.

From this experiment it is reasonable to conclude that the predominant mechanism for ultrasonic absorption is magnetoelastic in nature for our samples (binary alloy steels). Indeed there exists a theory for such loss (3,4) first postulated by W. Doring in the 1930's.

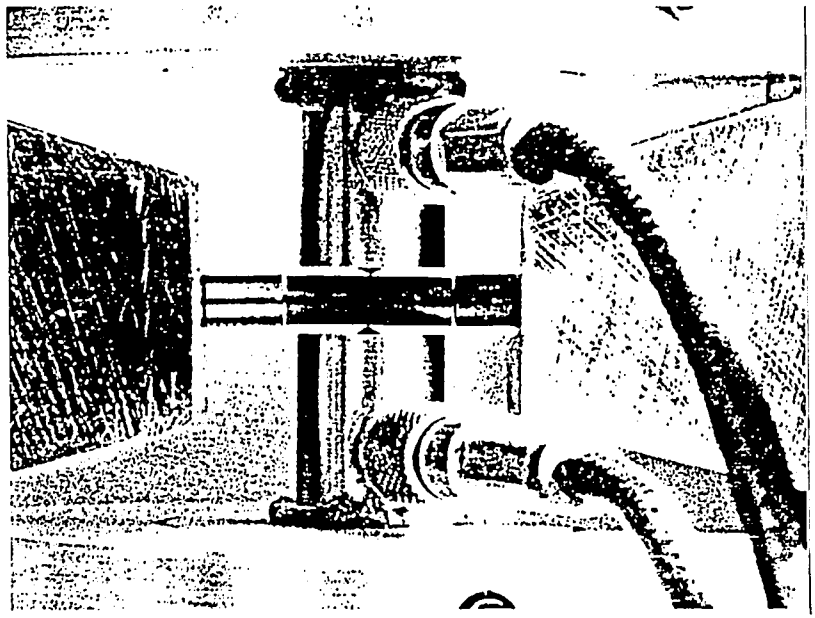

Figure 10. Configuration for Measurement under Magnetic Saturation.

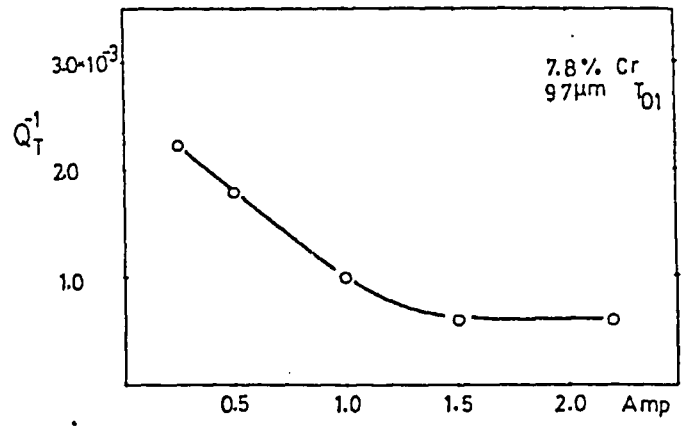

Figure 11. Decline of Q_t^{-1} in Fe-7.8 % Cr with Increasing Magnet Current.

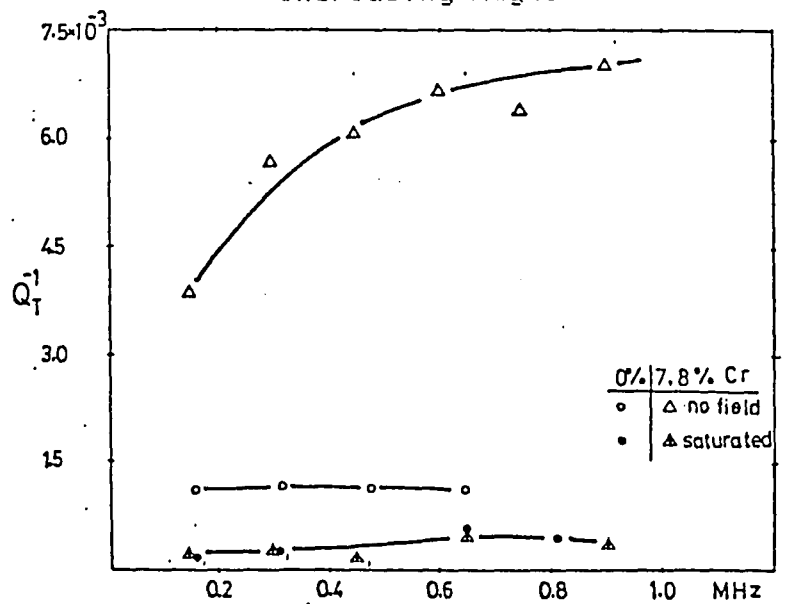

Figure 12. Q_t^{-1} in Fe and Fe-7.8 % Cr. No Magnetic Field and Magnetic Saturation.

Effect of Residual Strain

It was found that the ultrasonic absorption varies with a small amount of cold work and that the stress annealing does not necessarily reverse all the changes induced by the coldwork. This arises from the fact that there often exist differences in absorption between cylinders of the identical material (identical grain size and annealing). This difference is particularly pronounced between cylinders which are machined according to different procedures.

To illustrate this effect, an experiment was done on Fe- 7.8 % Cr cylinder which has been annealed at 800 $^{\circ}$C for one hour. The cylinder was put between the strictly parallel yaws of a hydraulic rig and compressed axially. After each compression (approximately 250 lb. increment in each step), absorption is measured. After the 500 lb. load, a 0.4 % reduction of height was measured. Figure 13 shows how Q_t^{-1} drops as coldwork is applied.

To further investigate the effect, a system was set up to simultaneously measure the initial magnetic permeability. In this case, a small axial hole was drilled through the cylinder, making it into a toroidal transformer core.

The induced secondary voltage was measured with sinusoidal primary excitation. From this voltage the initial permeability was calculated using the electromagnetic theory.

Figure 14 shows how the permeability drops with an increasing amount of coldwork (the same condition as in figure 13). By comparison, it can be seen that the permeability drops about proportional to the absorption. Therefore it can be concluded that the immediate cause for the drop of absorption with a small amount of coldwork is due to the drop in permeability, a result well compatible with Doring theory of magnetoelastic absorption.

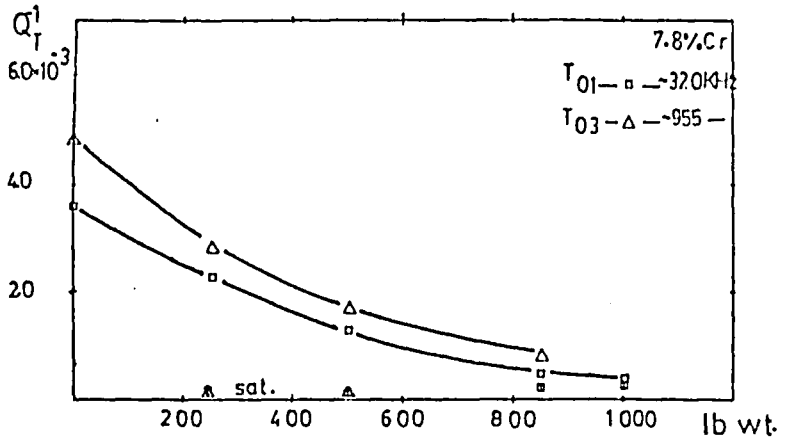

Figure 13. Drop of Q_t^{-1} after Successive Compression of Cylinder with Increasing Force. Two Frequencies. Also with Magnetic Saturation.

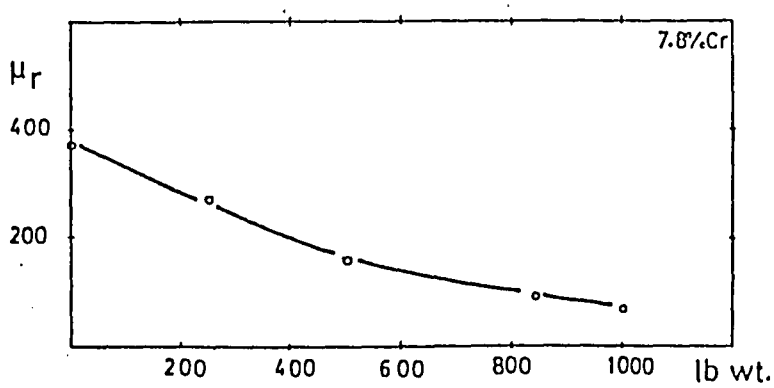

Figure 14. Drop of Initial Permeability after Successive Compression of Cylinder with Increasing Force.

IV. RESULTS AND DISCUSSIONS

The materials used in our experiment can be divided into two groups. The first group are steels with interstitial alloying elements (steels with C and P). The second group are steels with substitutional alloying elements (steels with Si, Mo, Cr). Both ultrasonic and mechanical data for each individual steel will be given separately. Before we present our results, some general introductory remarks are in order.

In ultrasonic attenuation measurements we observe that in most of the samples, the attenuations increase with the frequency in the lower frequency range, stay more or less constant for the intermediate frequency range and tend to drop at higher frequency, thus indicating a broad maximum. However exceptions are found in 1.5 % Si, 0.28 % P and 1.36 % Mo steels. 1.5 % Si and 0.28 % P steels have a sharper peak at a frequency which shifts with the grain size. In 1.36 % Mo steel samples of different grain sizes, a sharp peak at a lower frequency appears.

Ultrasonic measurements support the conclusion of Levy and Truell's (5) that shear modes induce much greater losses than the longitudinal modes in ferromagnetic materials. Also there seems to be an indication that the ultrasonic velocity increases with hardness in Fe-Cr, Fe-Mo, and Fe-P steels.

As far as the mechanical measurements are concerned, the data are in agreement with literature (6, 7, 8). The yield strength obeys the Hall-Petch relationship,

$$\sigma_{ys} = \sigma_o + k_y D^{-1/2}$$

where σ_{ys} is the yield strength.

σ_o is the frictional stress opposing the motion of dislocations.

k_y is the locking parameter (measure of the extent to which dislocations are piled up at barriers.

D is the mean ferrite intercept (a measure of average grain diameter).

Tensile strength and hardness also obey a similar relationship, but the relative influence of grain size is much less and depend more on the type and concentration of the alloying elements. The effect of alloying elements on yield stresses are given at the end of this chapter. It is noted that elongation and reduction of area are relatively insensitive to grain size.

Electrolytic Iron and 0.035 % C steel

Mechanical and ultrasonic measurements were made on four electrolytic iron samples having grain sizes 57, 86, 100, 120 μm and on four 0.035 % C steel having grain sizes 38, 56, 86, 97 μm . These cylinders were annealed at 500 ^{o}C.

Figures 15-16 show the attenuation data, Figure 17 shows the yield strength vs. grain size (Hall-Petch Plot) and Tables 3-4 give the mechanical test data.

Ultrasonic measurements on electrolytic iron and 0.035 % C steel failed to show any dependence of attenuation and velocity on grain size. Internal friction Q_t^{-1} is in the order of $1x10^{-3}$ and shear velocity is 3230 m/sec for electrolytic iron. 0.035 % C steel has the same magnitude for the internal friction Q_t^{-1} and a shear velocity of 3240 m/sec. In the experiment where measurements were made on electrolytic iron with applied magnetic field (magnetically saturated), Q_t^{-1} drops to $0.2x10^{-3}$. Ultrasonic properties of these samples are hardly distinguishable from each other.

Fe-Cr Steels

The mechanical and ultrasonic measurements were made on four 7.8 % Cr steel samples with grain sizes of 35, 57, 97, 138 μm and on three 3.8 % Cr steel samples with grain

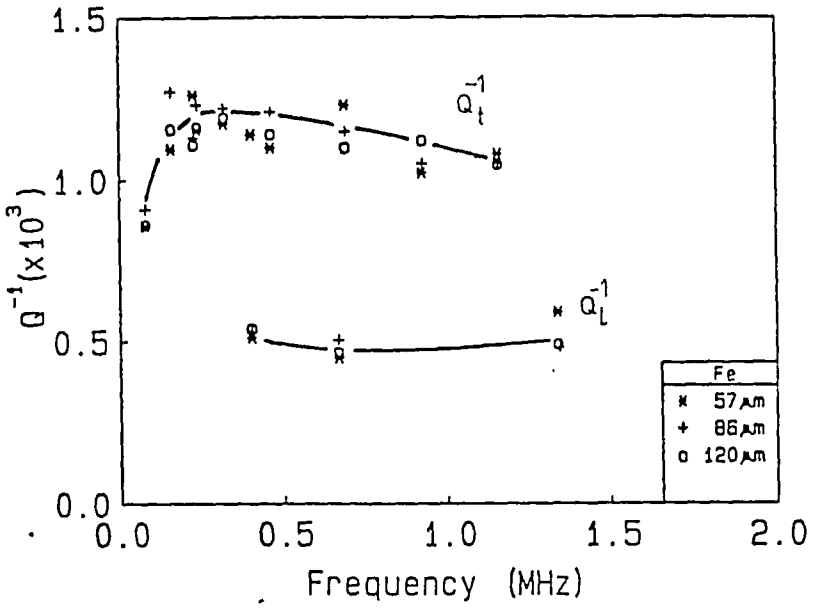

Figure 15. Q_t^{-1} and Q_l^{-1} in Electrolytic Iron, Varying Grain Size.

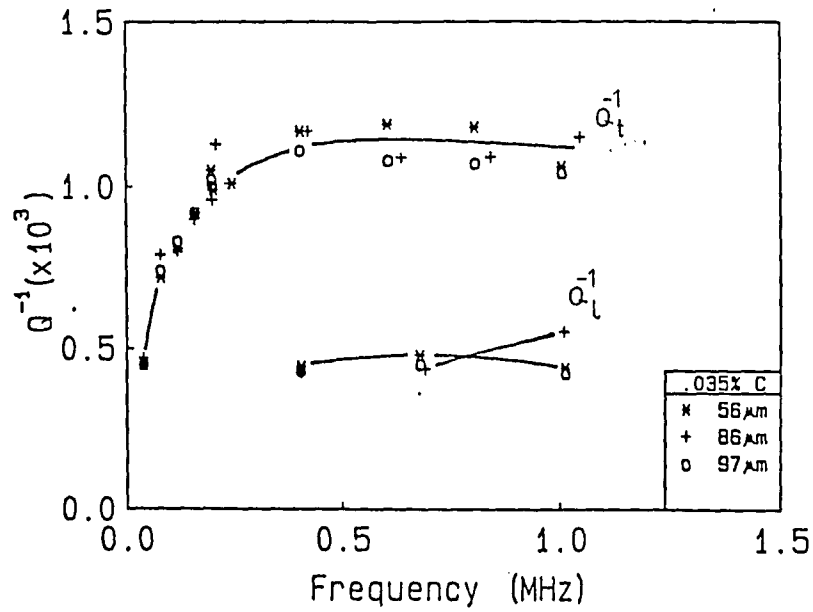

Figure 16. Q_t^{-1} and Q_l^{-1} in Fe-0.035 % C Steel, Varying Grain Size.

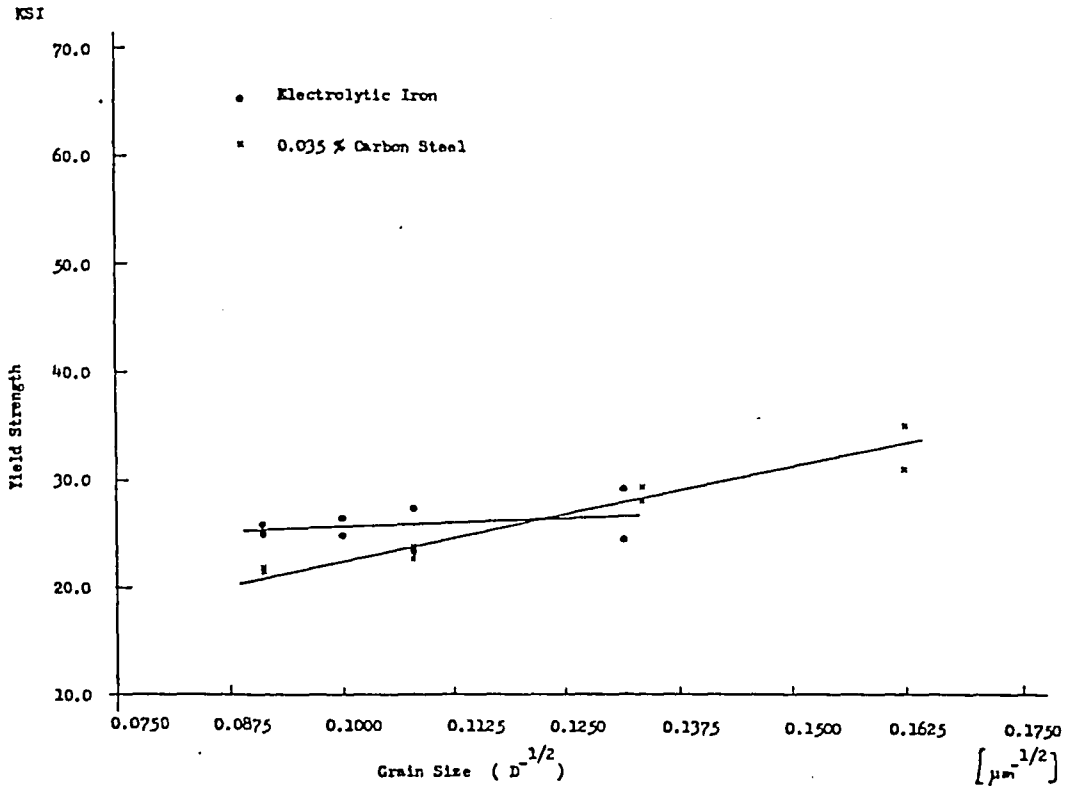

Figure 17. Curvefit to Hall-Petch Relation, Fe and Fe - 0.035 % C Steel.

Table 3. Mechanical Test Data for Electrolytic Iron.

Electrolytic Iron (48A)

Sample #	G.S. in mm	Y.S. ksi	U.T.S. ksi	% R.A.	%Elongation	Hardness R_E	Hardness R_B
18/1	0.057	28.95	36.25	-	-	67.47	18
18/2	0.057	24.12	37.30	75.72	56.60	68.37	20
20/1	0.086	23.08	37.12	75.98	51.54	67.97	19
20/2	0.086	27.13	36.59	77.98	54.88	67.73	19
22/1	0.100	26.05	35.69	75.24	53.75	58.13	02
22/2	0.100	24.84	36.18	77.66	49.80	60.60	06
26/1	0.120	24.92	36.74	78.94	49.93	57.63	02
26/2	0.120	25.72	36.66	78.81	47.80	60.17	05

Y.S. Yield strength

U.T.S. Ultimate tensile strength

%R.A. Percent reduction of area

R_E Rocwell E 100 kg load, 1/8" Ball, R_B Converted value from R_E using conversion table.

Table 4. Mechanical Test Data for Fe-0.035 % C Steel.

0.035 % C Steel (48B)

Sample #	G.S. in mm	Y.S. ksi	U.T.S. ksi	% R.A.	%Elongation	Hardness R_E	Hardness R_B
17/1	0.038	30.75	39.69	-	-	76.80	34
17/2	0.038	34.85	39.22	76.48	43.57	77.83	35
21/1	0.056	29.13	39.16	76.10	45.97	73.60	28
21/2	0.056	27.95	37.53	75.73	44.03	74.30	29
23/1	0.086	22.37	36.18	77.18	46.66	65.90	15
23/2	0.086	23.57	36.62	77.06	50.92	66.03	15
32/1	0.097	21.92	37.33	77.15	43.25	63.17	11
32/2	0.097	21.88	36.69	76.32	48.28	64.33	12

Y.S. Yield strength

U.T.S. Ultimate tensile strength

% R.A. Percent reduction of area

R_E Rocwell E 100 kg load, 1/8" Ball, R_B converted value from R_E using conversion table

sizes of 32, 51 and 161 μm. However, ultrasonic measurements were not made on the 3.8 % sample with 32 μm grain size, as this one could not be annealed at 800 ^{o}C without changing grain structure. Thus a stable absorption value was not reached. Ultrasonic attenuation measurements on these samples show that Q_t^{-1} is higher than the other alloy steels tested and ranges up to $7x10^{-3}$. Ultrasonic measurements were made on two sets of 7.8 % Cr samples (figures 18-19) Here attenuations strongly depend on residual stress and for this reason different samples yield different absorption. Ultrasonic measurements show that attenuation does not change appreciably as concentration changes from 3.8 to 7.8 % Cr (figure 20). However velocity of shear waves (3235 m/sec) is about 1.4 % higher in the 7.8 % Cr steel. The 3.8 % Cr steel indicates a shift in the peak with grain size.

The measurements on the longitudinal modes show that attenuations are much lower for these modes. Since only one measurement can be made from each cylinder and it is known that there is substantial difference in the residual stress betweeen the cyclinders, it is hard to draw any substantial conclusion from the shape of the Q_l^{-1} curve. Figure 21 shows an increase in shear velocity with hardness.

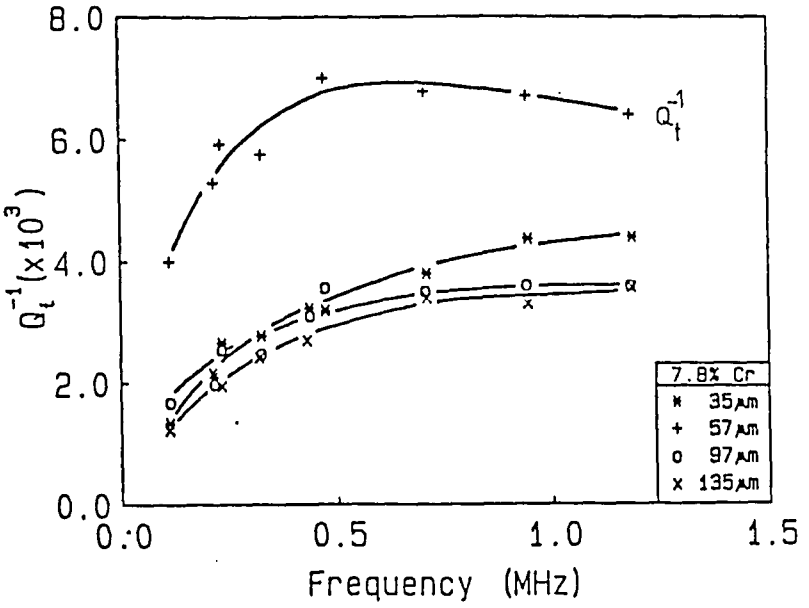

Figure 18. Q_t^{-1} in Fe-7.8 % Cr Steel, Varying Grain Size.

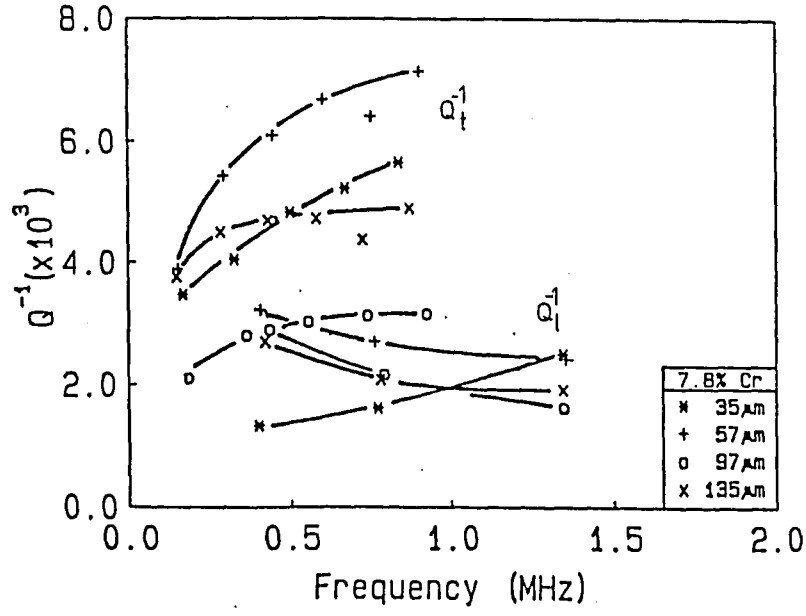

Figure 19. Q_t^{-1} and Q_l^{-1} in Fe-7.8 % Cr Steel Varying Grain Size, Alternate Specimen.

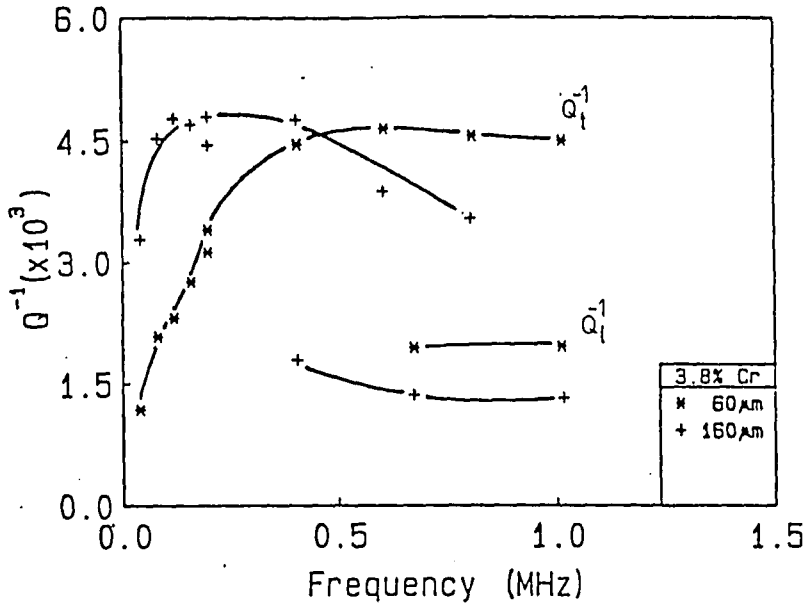

Figure 20. Q_t^{-1} and Q_l^{-1} in Fe-3.8 % Cr Steel, Varying Grain Size.

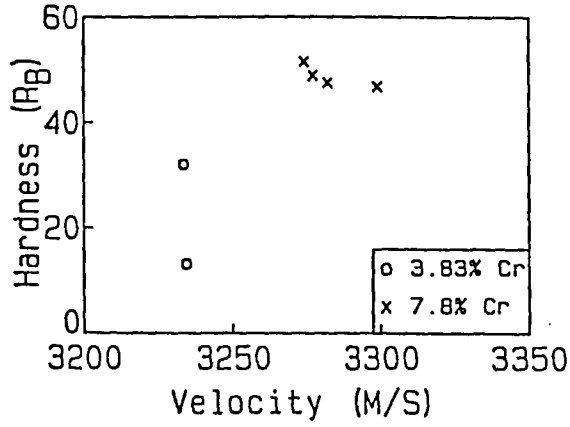

Figure 21. Hardness vs. Shear Velocity in Fe-Cr Steel

Mechanical measurements do no show an appreciable difference in the in yield strength between 7.8 % and 3.8 % Cr (figure 22). However there is an increase in hardness as the concentration increases (Tables 5-6). In both samples the yield strength depends on grain size, however, the dependence of hardness on grain size is not distinct.

Fe-Si Steel

Mechanical and ultrasonic measurements were made on Si steels having concentrations of 1.5 % and 0.8 %. Mechanical measurements show that in 1.5 % Si steel, the yield strength depends very strongly (figure 25) on the grain size of the samples (indicating a large locking parameter, Ky). However, the hardness of these samples hardly depends on the grain size (Tables 7-8). Ultrasonic measurements show that the frequency at which attenuation is maximum depends strongly on the grain size. Such distinct relationship does not exist in 0.8 % Si steel (figures 23-24). In Si steels, the reproducibility of ultrasonic data is not very good, even though all 1.5 % Si samples were annealed at 800 ^{o}C. The 0.8 % Si samples were annealed at 500 ^{o}C. Shear velocity (3240 m/sec) is slightly higher in the 0.8 % Si steel.

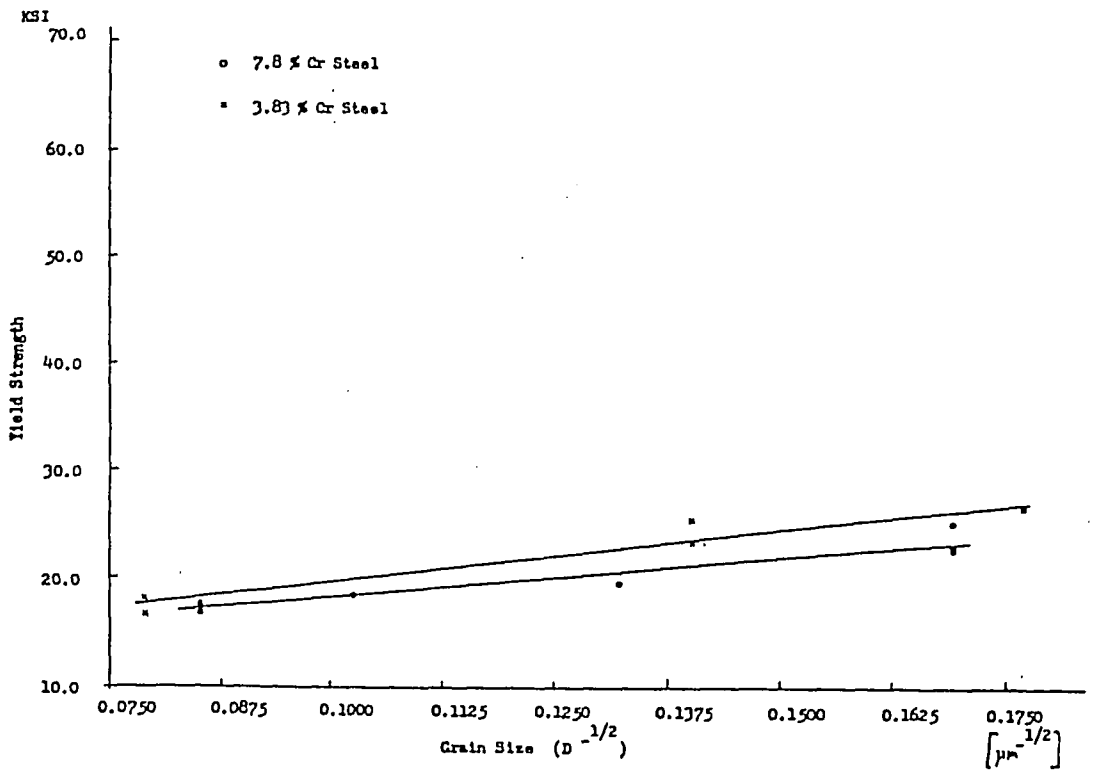

Figure 22. Curvefit to Hall-Petch Relation, Fe-3.8 % Cr and Fe-7.8 % Cr Steels.

Table 5. Mechanical Test Data for Fe-3.8 % Cr Steel.

3.87 % Cr Steel (T025)

Sample #	G.S. in mm	Y.S. ksi	U.T.S. ksi	% R.A.	% Elongation	Hardness R_B
35/1	0.032	26.94	41.42	79.14	48.93	32.30
35/2	0.032	26.45	41.94	79.77	47.69	30.85
37/1	0.051	25.49	41.18	77.70	36.29	32.48
37/2	0.051	23.42	39.37	79.07	38.34	31.85
36/1	0.161	18.18	38.64	74.13	42.24	11.80
36/2	0.161	16.77	37.68	72.67	45.31	14.65

Y.S. Yield strength

U.T.S. Ultimate tensile strength

% R.A. Percent reduction of area

R_B Rockwell B, 100 kg load, 1/16" Ball

Table 6. Mechanical Test Data for Fe-7.8 % Cr Steel.

7.8 % Cr Steel (54B)

Sample #	G.S. in mm	Y.S. ksi	U.T.S. ksi	% R.A.	% Elongation	Hardness R_B
12A/1	0.035	22.84	45.22	80.81	49.85	52.0
12A/2	0.035	22.90	44.27	82.21	48.87	51.7
12	0.035	25.28	47.52	79.68	48.87	51.5
15	0.057	19.69	45.22	77.33	48.33	48.9
13	0.095	18.46	44.46	74.96	46.38	46.8
14	0.138	17.61	47.17	75.65	40.62	47.5
14A/1	0.138	16.85	41.73	76.07	40.62	45.5
14A/2	0.138	17.05	42.64	75.59	40.70	47.0

Y.S. Yield strength

U.T.S. Ultimate tensile strength

% R.A. Percent reduction of area

R_B Rockwell B, 100 kg load, 1/16" Ball

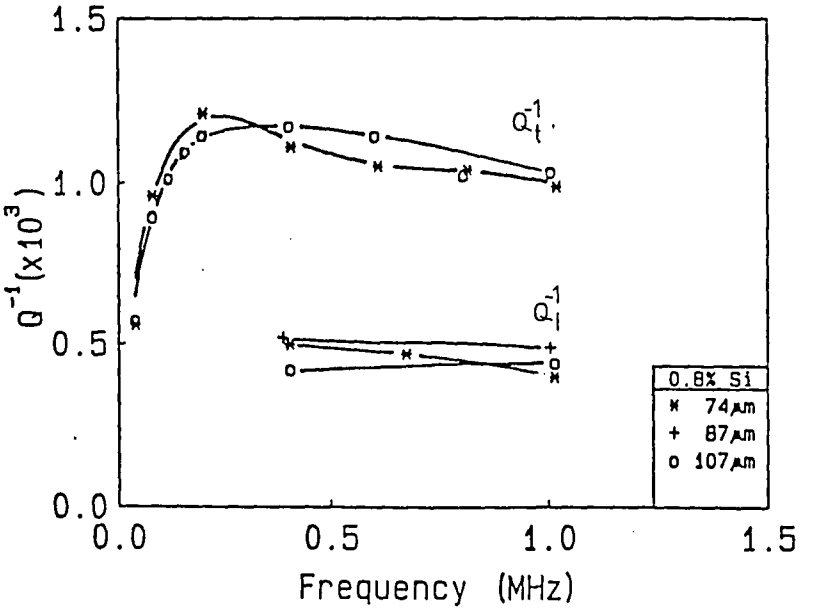

Figure 23. Q_t^{-1} and Q_l^{-1} in Fe-0.8 % Si Steel, Varying Grain Size.

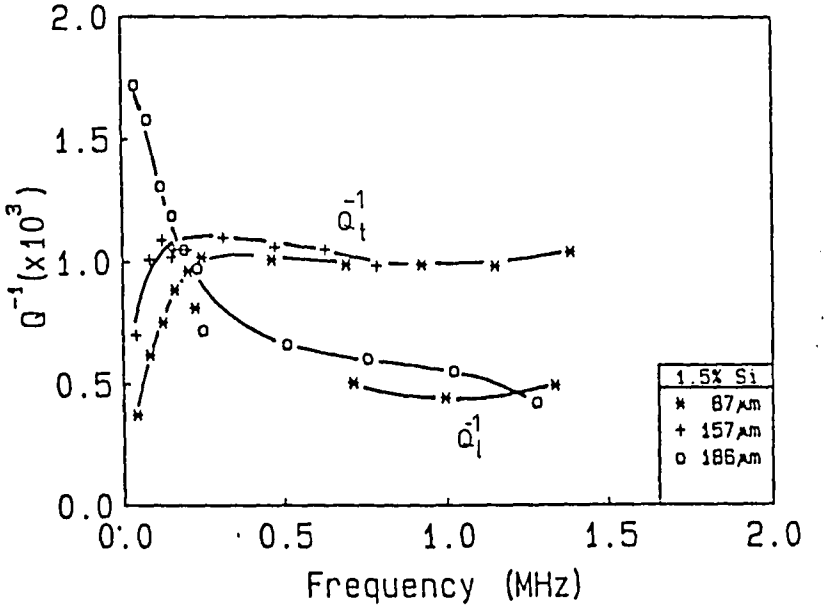

Figure 24. Q_t^{-1} and Q_l^{-1} in Fe-1.5 % Si Steel, Varying Grain Size.

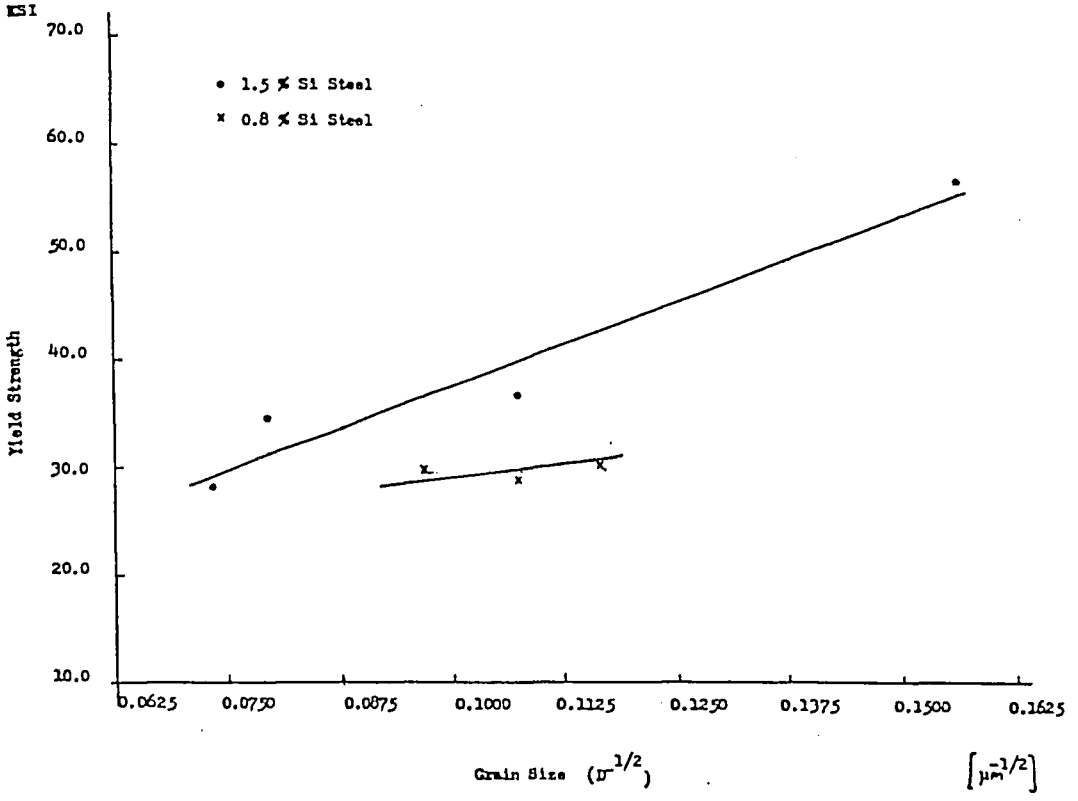

Figure 25. Curvefit to Hall-Petch Relation, Fe-0.8 % Si and Fe-1.5 % Si Steels.

Table 7. Mechanical Test Data for Fe-0.8 % Si Steel.

0.8 % Si Steel (T024)

Sample #	G.S. in mm	Y.S. ksi	U.T.S. ksi	% R.A.	% Elongation	Hardness R_B
54	0.074	30.18	50.30	83.14	49.74	50.25
53	0.087	28.73	40.32			45.53
52	0.107	29.80	49.49	83.16	43.67	48.50

Y.S. Yield strength

U.T.S. Ultimate tensile strength

% R.A. Percent reduction of area

R_B Rockwell B 100 kg load, 1/16" Ball

Table 8. Mechanical Test Data for Fe-1.5 % Cr Steel.

1.5 % Si Steel (50A)

Sample #	G.S. in mm	Y.S. ksi	U.T.S. ksi	% R.A.	% Elongation	Hardness R_B
24	0.041	56.45	67.20	62.45	28.77	83.17
19	0.087	36.51	57.55	75.30	44.85	65.90
27	0.157	34.46	55.89	66.41	42.42	66.76
25	0.186	28.11	50.36	57.18	38.58	63.93

Y.S. Yield strength

U.T.S. Ultimate tensile strength

% R.A. Percent reduction of area

R_B Rockwell B 100 kg load, 1/16" Ball

Fe-Mo Steel

Mechanical and ultrasonic measurements were made on two Mo steel samples with 3.6 % and 1.5 % Mo. Mechanical measurements show that the yield strength changes with grain size (figure 29), but the hardness does not (Tables 9-10). Conversely with the change in concentration, the yield strength does not change but the hardness does (Tables 9-10).

The ultrasonic attenuation measurements show that the 3.6 % Mo steel shows a broad peak, however, the 1,36 % Mo samples show a sharper peak at a lower frequency (figures 26-27). The Q_t^{-1} of samples of both concentrations are comparable. The shear velocity (3160 m/sec) increases slightly with the concentration of Mo. A plot of shear velocity versus hardness are given in figure 28.

Fe-P steel

Mechanical and ultrasonic measurements were made on two P steel samples with 0.28 % and 0.082 % P. The mechanical measurements show that for 0.28 % P the ky value (locking parameter is large (figure 33) and ultrasonic measurements show that the frequency at which attenuation is maximum depends on the grain size (figures 30-31). This correlation is similar to that of 1.5 % Si steel samples. However, the lower concentraiton of P failed to show any

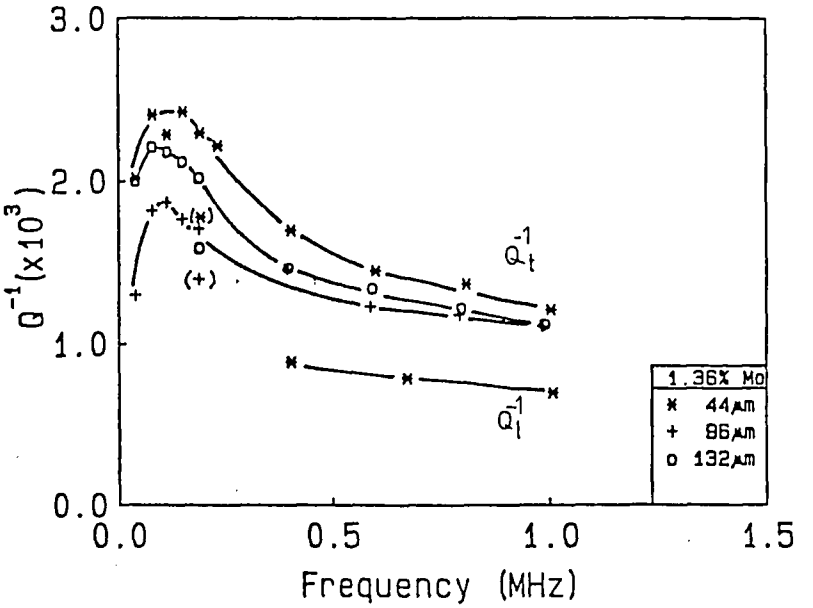

Figure 26. Q_t^{-1} and Q_l^{-1} in Fe-1.5 % Mo Steel, Varying Grain Size.

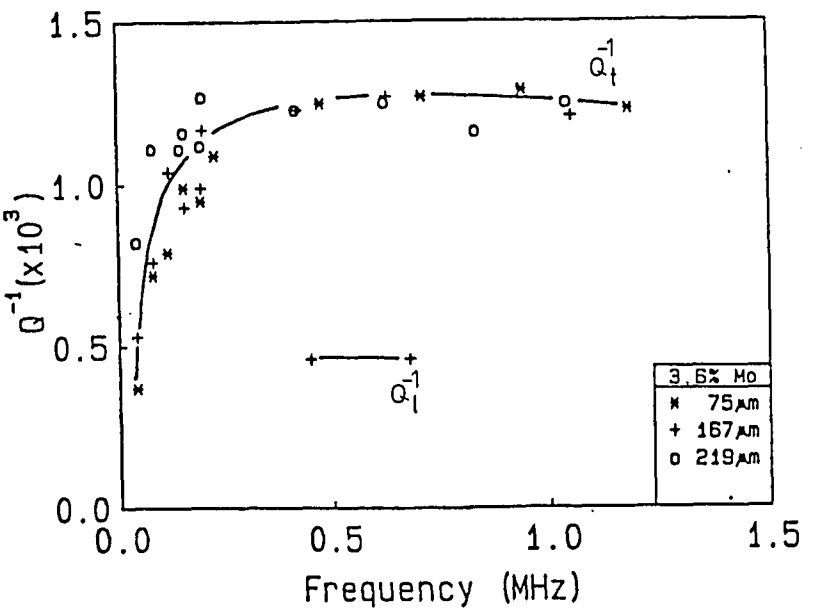

Figure 27. Q_t^{-1} and Q_l^{-1} in Fe-3.6 % Mo Steel, Varying Grain Size.

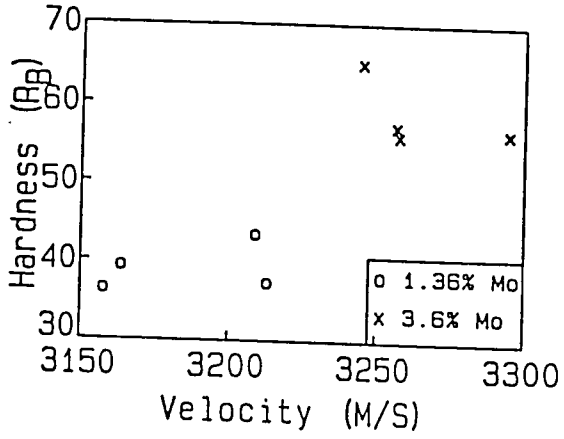

Figure 28. Hardness vs. Shear Velocity in Fe-Mo Steel.

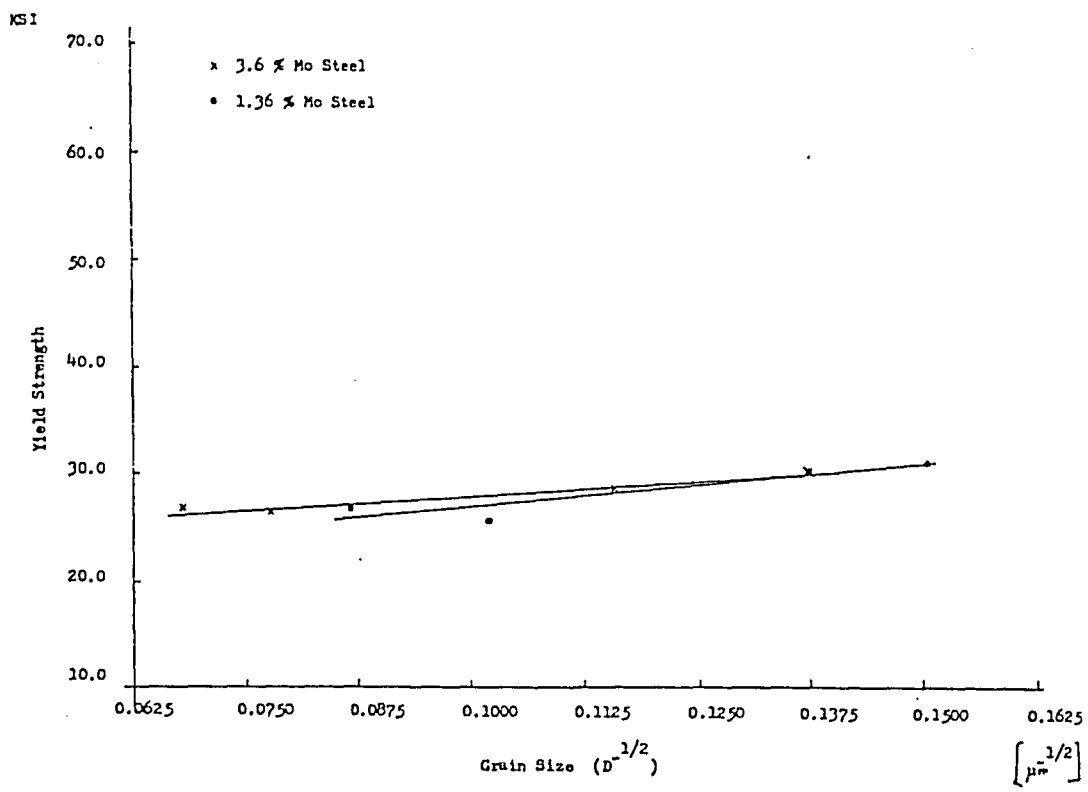

Figure 29. Curvefit to Hall-Petch Relation, Fe-1.36 % Mo and Fe-3.6 % Mo Steels.

Table 9. Mechanical Test Data for Fe-1.36 % Mo Steel.

1.36 % Mo Steel (T023)

Sample #	C.S. in mm	Y.S. ksi	U.T.S. ksi	% R.A.	%Elongation	Hardness R_B
45	0.044	30.80	44.66	82.10	44.66	43.45
44	0.053	29.92	44.32	83.12	42.79	37.30
47	0.096	25.35	44.27	79.84	26.68@	39.28
46	0.132	26.68	44.50	81.34	41.29	36.35

Y.S. Yield strength

U.T.S. Ultimate tensile strength

% R.A. Percent reduction of area

R_B Rockwell B, 100 kg load, 1/16" Ball

Table 10. Mechanical Test Data for Fe-3.6 % Mo Steel.

3.6 % Mo Steel (51A)

Sample #	C.S. in mm	Y.S. ksi	U.T.S. ksi	% R.A.	% Elongation	Hardness R_B
28	0.053	30.16	52.59	53.95	33.06	65.00
29	0.075	26.84	50.15	65.60	33.92	55.90
30	0.167	26.23	49.69	66.35	37.38	56.43
31	0.219	26.73	49.53	68.24	37.92	57.07

Y.S. Yield strength

U.T.S. Ultimate tensile strength

%R.A. Percent reduction of area

R_B Rockwell B 100 kg load, 1/16 " Ball

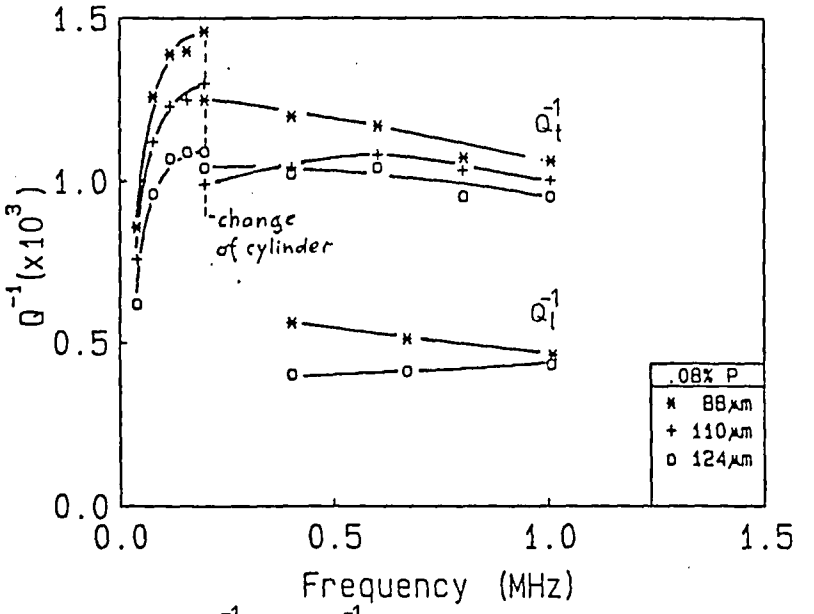

Figure 30. Q_t^{-1} and Q_l^{-1} in Fe-0.08 % P Steel, Varying Grain Size.

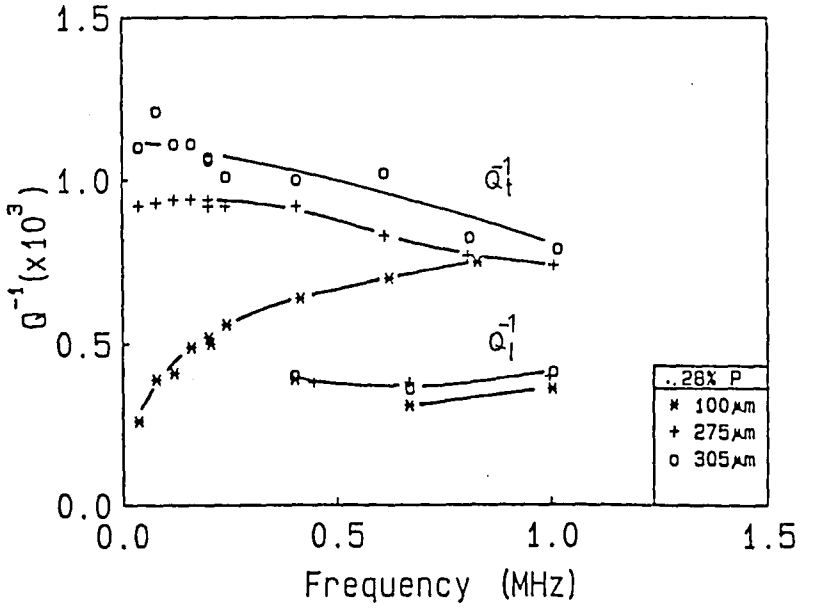

Figure 31. Q_t^{-1} and Q_l^{-1} in Fe-0.28 % P Steel, Varying Grain Size.

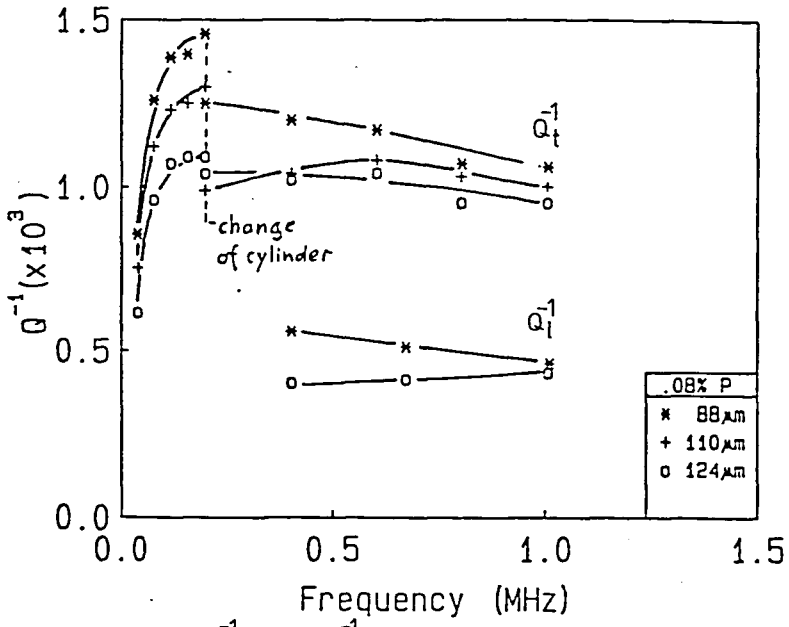

Figure 30. Q_t^{-1} and Q_l^{-1} in Fe-0.08 % P Steel, Varying Grain Size.

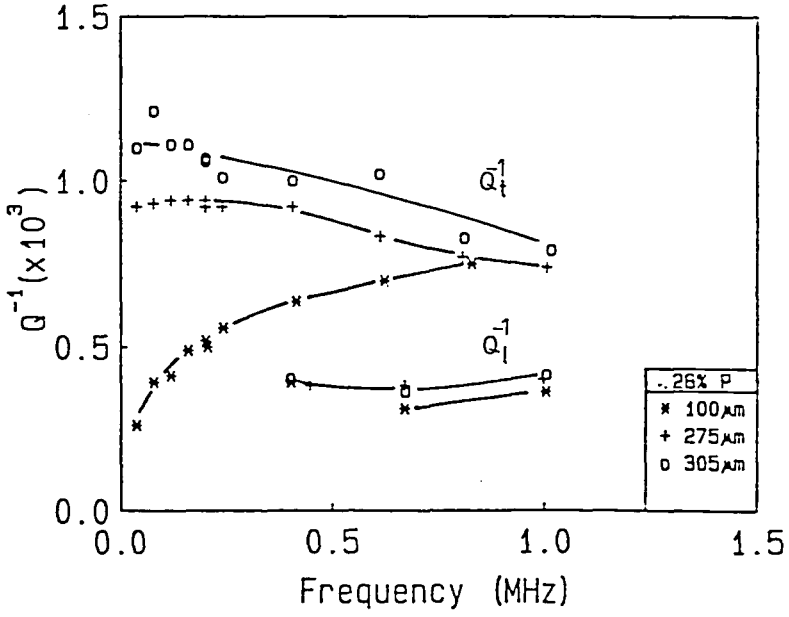

Figure 31. Q_t^{-1} and Q_l^{-1} in Fe-0.28 % P Steel, Varying Grain Size.

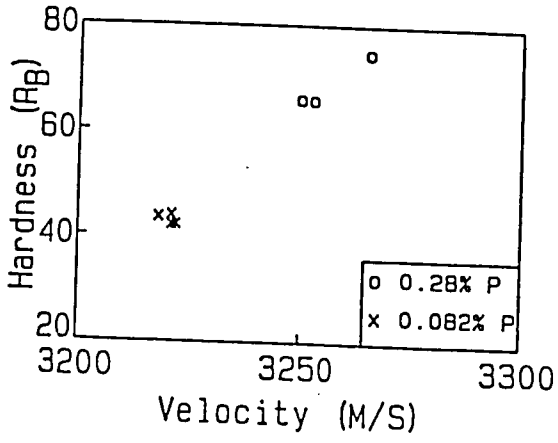

Figure 32. Hardness vs. Shear Velocity in Fe-P Steel.

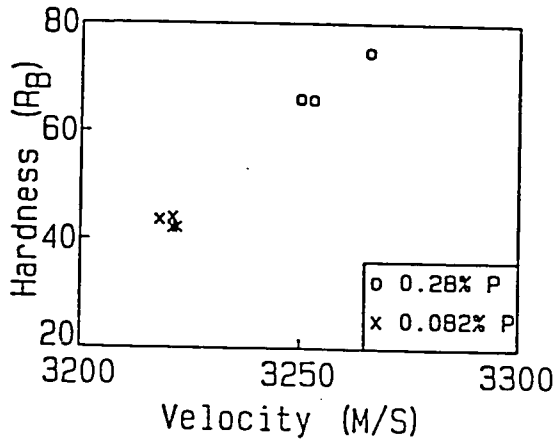

Figure 32. Hardness vs. Shear Velocity in Fe-P Steel.

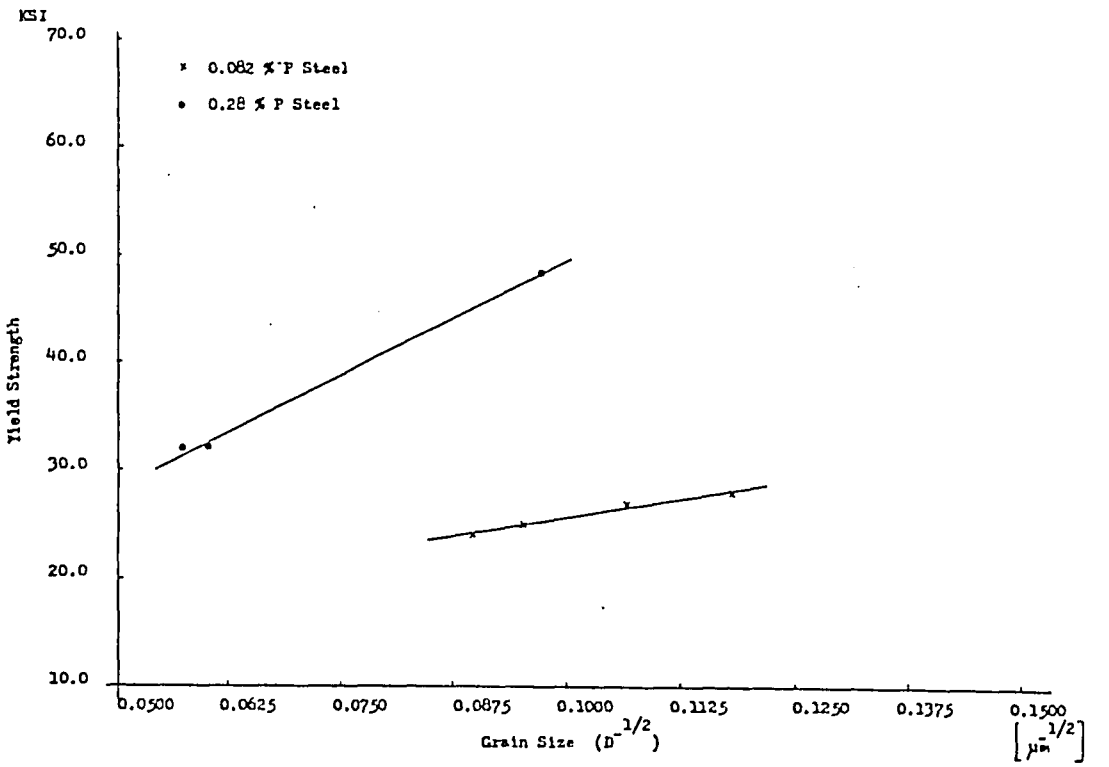

Figure 33. Curvefit to Hall-Petch Relation, Fe-0.08 % P and Fe-0.28 % P Steels.

Table 11. Mechanical Test Data for Fe-0.08 % P Steel.

0.082% P Steel (T022)

Sample #	G.S. in mm	Y.S. ksi	U.T.S. ksi	% R.A.	% Elongation	Hardness R_B
51	0.072	28.00	47.86	70.84	46.58	42.13
50	0.088	27.16	46.28	70.22	47.01	43.50
49	0.110	25.15	46.78	73.59	45.68	43.93
48	0.124	24.24	46.46	74.67	46.20	42.03

Y.S. Yield strength

U.T.S. Ultimate tensile strength

%R.A. Percent reduction of area

R_B Rockwell B 100 kg load, 1/16 " Ball

Table 12. Mechanical Test Data for Fe-0.28 % P Steel.

0.28 % P Steel (52A)

Sample #	G.S. in mm	Y.S. ksi	U.T.S. ksi	% R.A.	%Elongation	Hardness R_B
38	0.106	48.39	62.50	77.08	43.18	74.68
39	0.277	32.25	55.98	77.21	43.78	65.68
40	0.306	32.32	56.16	76.50	44.23	65.85

Y.S. Yield strength

% R.A. Percent reduction of area

U.T.S. Ultimate tensile strength

R_B Rockwell B, 100 kg load, 1/16" Ball

of such correlation. With increase in concentration the yield strength, tensile strength, hardness and shear velocity changed (figure 32 and Tables 11-12). For 0.08 % P steel, the correlation between hardness and grain size is poor.

Effect of Alloying Elements on Yield Stresses of Steels

One way that alloying elements have effects on yield stresses is by solid solution hardening. This can be achieved by either interstitial or substitutional alloying elements. As previously mentioned, the materials in our experiment can be divided into two groups. The first group are steels with interstitial alloying elements (steels with C and P). The second group are steels with substitutional alloying elements (steels with Si, Mo, Cr).

From the experimental data it can be concluded that :

1. The substitutional alloying elements (group 2) have a relatively small solid solution hardening effect. The increment in yield stress with increasing the percentage of alloying elements is relatively small. For example, the increment of chromium from 3.8 wt. % to 7.8 wt. % or increment of molybdenum from 1.3 wt. % to 3.6 wt. % in these two steels has little effect on the yield stresses.

2. In the interstitial alloy steels (group 1), the solid solution hardening effect is very large. A small increment in percent alloying elements has a large effect on the increment of yield stresses. From the experimental data, an increase of phosphorus by 0.2 wt. % increases the yield stress by almost 20 ksi.

3. The dependence of yield stresses on grain size is not quite pronounced in steels with substitutional alloying elements as compared with the alloys with interstitial alloying elements. This can be seen from the slope of the Hall-Petch plot (the ky value).

4. The slope of the Hall-Petch plot (the ky value) increases with the increase of wt. percent alloying elements. The increment is by far more effective in steels with interstitial alloying elements than in steels with substitutional alloying elements.

In order to explain the above statements it is necesasary to understand the theory of yielding. According to Cottrell (9) the solute atoms tend to diffuse to dislocations because this lowers the strain energy of the system. The dislocations are then pinned by an atmosphere of solute atoms. Yielding occurs when the applied stress is high enough to unpin the dislocations by pulling away from their atmosphere. Thus the statements one and two can be explained by the fact that interstitial

alloying elements are more effective in pinning dislocations than substitutional alloying elements. The effects of each individual alloying elements on solid solution hardening were studied in detail by K. J. Irvine and F. B. Pickering (6).

The slope of the Hall-Petch plot (the ky value) is a measure of the pinning dislocations, and is related to the number of dislocations released into a slip band when a dislocation source is unpinned (10, 11, 12). It is therefore dependent on the type and concentration of alloying elements present in the material. In substitutional alloying elements the pinnig effects are small, thus the ky value and its increment with the increase of the wt. percent alloying elements are small. On the other hand the pinning effects by interstitial alloying elements are large. In this case the increment of ky value with the wt. percent alloying elements is more pronounced as compared with the case of substitional alloying elements. The above discussions can be used to explain statements three and four. It is difficult, however, to provide a quantitative analysis of the Hall-Petch relation based on the present data.

V. CONCLUSIONS

1. It was found that at room temperature and in the frequency range of 100 KHz to 1.5 MHz the predominant mechanism for ultrasonic absorption is magnetoelastic in nature (micro-eddycurrent loss) for our samples (binary alloy steels). This is well supported by the theory of micro-eddycurrent damping which was first postulated by W. Doring in the 1930's (3).

2. The ultrasonic absorption is strongly influenced by the residual strain (coldwork effect). From our experimental data, it can be concluded that the immediate cause for the drop of absorption with coldwork is due to the drop in permeability.

3. The ultrasonic absorption is mostly due to the shear viscosity coefficent which is found to be much larger than the bulk viscosity coefficient. This finding supports the conclusion of Levy and Truell's (5).

4. Some characteristic grain size dependence of absorption exists in Fe-Si and Fe-P alloy steels. In these steels the frequency at which attenuation is maximum depends on the grain size.

5. In the Fe-Cr, Fe-Mo and Fe-P alloy steels, there is a correlation between shear velocity and hardness.

6. From the mechanical data, the relation between grain size and the yield strength can be established (Hall-Petch relation). Tensile strength and hardness obey a similar relationship, but the relative influence of grain size is much less and depend more on the type and concentration of the alloying elements. The elongation and reduction of area are relatively insensitive to grain size.

7. As far as application to nondestructive evaluation of mechanical properties is concerned, our findings are not very encouraging. Measurements of absorption certainly ranks far behind scattering measurements. However, knowledge of the absorption background is an important ingredient in interpreting scattering data.

REFERENCES

1. N. Eberhardt, A. Tverdokhlebov, "A Resonance Method for Measurement of Longitudinal and Transverse Ultrasonic Wave Velocities and Their Attenuations," In: Review of Progress in Quantitative Nondestructive Evaluation, p. 639-646, Vol. 1, Plenum Press, New York, 1982.
2. A. Tverdokhlebov, N. Eberhardt, "An Improved Approach to the Computation of Sonic Resonant Frequencies of Cylinders,", Ibid. p. 647-651.
3. R. Becker, W. Doring, "Ferromagnetismus," p. 379, Springer, 1939.
4. W. P. Mason, Phys. Rev. Vol. 83, p. 683, 1951.
5. S. Levy, R. Truell, "Ultrasonic Attenuation in Magnetic Single Crystals," Rev. of Modern Physic, Vol. 25, No. 1, p. 140-145, 1953.
6. K. J. Irvine & F. B. Pickering, JISI, p. 944-959, November 1963.
7. Edgar C. Bain, Harold W. Paxton, "Alloying Elements in Steel," p. 270, 1966.
8. Gladman T.,et al., "Work Hardening of Low-Carbon Steels," JISI, Vol. 208, p.172, 1970.
9. A. H. Cottrell, " Dislocations and Plastic Flow in Crystals," p. 99-150, 1953.

10. A. H. Cottrell, Trans., AIME, p. 192-203, April 1958.

11. A. A. Johnson, Acta Met., p. 737-740, October 1960.

12. J. C. M. Li & Y. T. Chou, Met. Trans.,
p. 1145-1159, May 1970.

VITA

Surin Tantitharoenkiat, son of Mr. Tan Keng Choon and Mrs. Suchinda Tantitharoenkiat, was born on December 24, 1957, in Bangkok, Thailand. He atteneded Triam Udom Suksa school in Bangkok, Thailand, and received his High School Diploma in 1975. In June, 1975, he entered Chulalongkorn University in Bangkok, Thailand, and received the degree of Bachelor of Science in March, 1979. In September 1979, he entered Auburn University in Auburn, Alabama. He graduated in 1981 with a Master of Science in Mechanical Engineering. Since August 1981, he has been a graduate student in the Department of Metallurgy and Materials Engineering at Lehigh University, Bethlehem, Pennsylvania.